JOURNAL OF OPTOELECTRONICS AND ADVANCED MATERIALS Vol. 8, No. 1, February 2006, p. 95 - 98

Structural and spectroscopical characterization of RE^{3+}(RE = Er, Eu, Tb) doped nanocrystalline YAG produced by a sol-gel method

A.-M. CHINIE*, A. STEFAN, S. GEORGESCU, O. TOMA, ELENA BORCA[a], M. BERCU[a]
National Institute for Lasers, Plasma and Radiation Physics, Bucharest-Magurele, Romania
[a]*Faculty of Physics, University of Bucharest, Bucharest, Romania*

Nanocrystalline YAG powders doped with Er^{3+}, Eu^{3+} or Tb^{3+} were synthesized through a citrate-nitrate sol-gel process. Thermal treatments were applied at successively increasing temperatures in the interval 600-1400 ºC. The structural transformations were monitored by XRD, FT-IR and optical spectroscopy. A pure garnet phase was observed for annealing temperatures higher than 930 °C.

(Received October 14, 2005; accepted January 26, 2006)

Keywords: Nanocrystals, YAG, Eu^{3+}, Er^{3+}, Tb^{3+}, Sol-gel method

1. Introduction

Yttrium aluminates based on the system Y_2O_3–Al_2O_3 are promising materials with regard to their optical, mechanical, chemical, and thermal properties The yttrium aluminum garnet (YAG – $Y_3Al_3O_{12}$) crystallizes in the cubic form and exhibits outstanding properties when doped with lanthanide or transition elements. Usual applications include laser active media and phosphors. Nd:YAG is the most widely used solid-state active medium and, recently, highly efficient ceramic Nd:YAG active media were produced [1]. YAG:Eu^{3+} and YAG:Tb^{3+} are, respectively, well-known red and green phosphors [2,3], while YAG:Er^{3+} (co-doped with Yb^{3+}) is used as up-conversion phosphor [4].

The solid-state synthesis of YAG ceramics from aluminum and yttrium oxides requires high sintering temperatures (> 1600 °C) [5]. In such conditions, it is difficult to control the homogeneity and purity of YAG powders. An alternative synthesis approach is the sol-gel method [6]. This method allows for preparation of high-purity single-phase YAG at significantly lower temperature.

In this paper we use a citrate-nitrate sol-gel method [7] to prepare rare earth (Er, Eu, Tb) doped YAG nanocrystals. The transition from the amorphous to the garnet phase and the change of the crystallite size induced by the thermal treatment were monitored by X-Ray Diffraction (XRD), Fourier Transform InfraRed (FT-IR) spectroscopy and optical spectroscopy.

2. Experimental

Aqueous solutions of $Y(NO_3)_3 \cdot 5H_2O$ and $Al(NO_3)_3 \cdot 9H_2O$ were mixed in a molar ratio 3:5 (Y:Al). For the rare-earth doped YAG, Al, Y and rare earth (RE) nitrates were mixed in a molar ratio according to the formula $Y_{3-x}RE_xAl_5O_{12}$. The mixture was added to a citric acid solution ($C_6H_8O_7 \cdot H_2O$) 2M, in molar ratio citric acid:nitrates of 3:1. The sol transition into transparent gel, with small amount of water, takes place around 80 ºC. The following compositions, corresponding to: YAG:Er(1at.%), YAG:Eu(3 at. %) and YAG:Tb(10 at.%), were synthesized.

Thermal treatments were applied at successively increasing temperatures in the interval 600-1400 ºC. The gel was decomposed at 600 ºC for 6 h to obtain a black fluffy powder in an amorphous state. This powder was calcinated at 850 ºC achieving a white amorphous powder. After a thermal treatment at 930 ºC, pure crystalline YAG phase was obtained.

XRD measurements were performed at room temperature on a TUR M-62 diffractometer (on line with a PC) using Co K_α radiation (λ = 1.7902 Å). Infrared spectra were recorded on a SCIMITAR type FT-IR spectrometer (model 2001, Digilab, SUA) using the KBr pellet technique. The experimental apparatus used for absorption and fluorescence in the visible domain consisted of a GDM 1000 double monochromator equipped with an S-20 photomultiplier in photon counting configuration and a TURBO MCS scaler in line with a computer. Fluorescence was excited with a Xenon lamp equipped with suitable optical filters. For absorption and fluorescence in the visible domain, the powder was placed in a quartz cuvette.

3. Results and discussion

3.1. X-ray diffraction

X-ray diffractograms for YAG:Er, YAG:Eu and YAG:Tb powder samples annealed at various temperatures were recorded. Regardless the dopant, the diffraction

patterns showed the same evolution of crystalline structure of the YAG:RE powders during the annealing process. As an example, XRD patterns of the precursor and powders fired at various temperatures are shown in Fig. 1 together with diffraction pattern of a bulk crystal (YAG). No diffraction peaks were observed for temperatures up to 900 ºC. For samples annealed at 930 ºC or higher temperatures only the diffraction lines characteristic for the YAG phase were recorded.

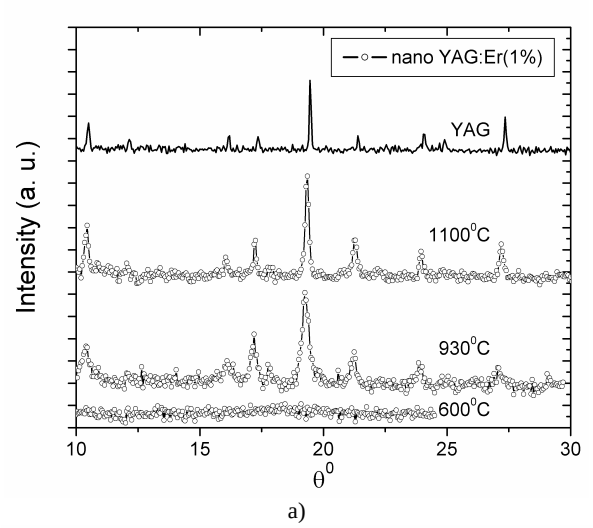

Fig. 1. a) XRD patterns of precursor and nanopowders of YAG:Er(1%) annealed at various temperatures; b) diffraction pattern for YAG:Eu(3%) nanopowder annealed at 930 °C and for a bulk crystal of YAG (as reference).

Assuming a simplified (Lorentzian) model for size-broadened diffraction line profile, the apparent volume-weighted crystallite size (D_V) was estimated from Scherrer's equation [8]. A correction for instrumental broadening of diffraction lines was introduced using Si powder as standard sample. In this analysis we neglected the strain–broadening of the profile (due to the lattice distortion). In this rough approximation, the crystallite size can be overestimated. Besides these peculiarities, the apparent domain size derived from the FWHM of line profile can be used to study changes in crystallite size due to the annealing treatment of YAG nanopowders.

In our YAG:RE nanopowders obtained by the sol-gel method a monotonous increase of the crystallite size with annealing temperature was obtained (Fig. 2). The smallest crystallites (corresponding to 930 ºC annealing temperature) are of ~25 nm while the largest (treated at 1300 ºC) measure ~82 nm.

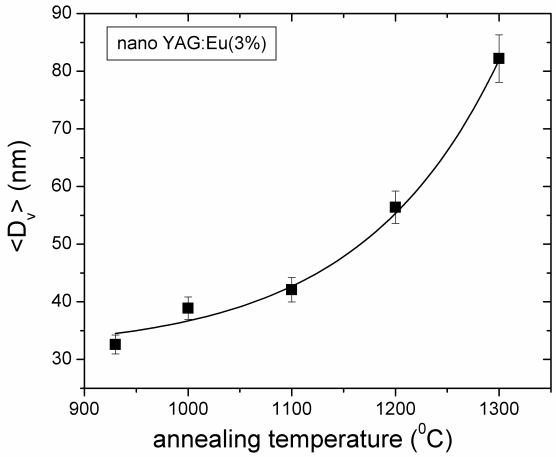

Fig. 2. Effect of annealing temperature on apparent average crystallite size for YAG:Eu(3%) nanopowder. The continuous line is only guide for the eyes.

3.2. FT-IR spectroscopy

The FT-IR measurements were found to be consistent with the YAG phase crystallization process observed by X-ray diffraction. Fig. 3 shows the FT-IR spectra of the precursor and powders synthesized at different temperatures for YAG:Er(1%) (left) and YAG:Eu(3%) (right). The samples annealed at temperatures higher than 900 °C show high absorption in the region 400-900 cm^{-1}, revealing the transition from amorphous phase of precursor to the crystalline phase of YAG. The absorption bands observed in this region are characteristic to the metal-oxygen stretching vibrations [9]. In YAG:RE samples the transition from amorphous to crystalline phase takes place in a narrow interval of temperatures (between 900 and 930 ºC).

The absorption in the region of 1400-1700 cm^{-1} observed in spectra recorded on the samples synthesized at temperatures lower then 900 ºC indicate the presence of the impurities adsorbed on the large surface of nanopowders (not fully decomposed nitrate, CO from not burned organic precursors and O-H) [10]. The absorption in this range almost disappears in the nanocrystalline powders obtained after annealing at T > 900 °C.

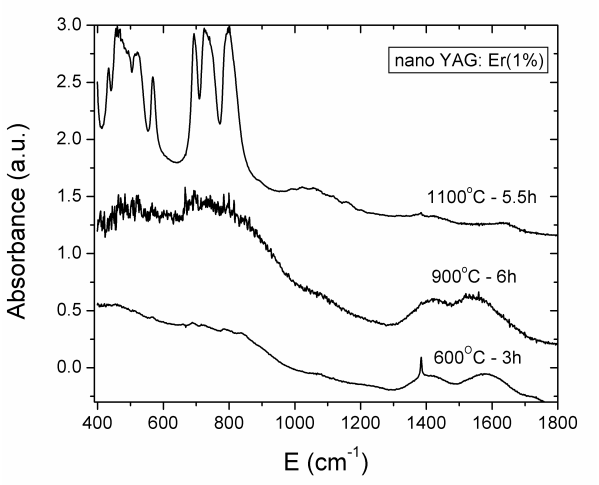

a)

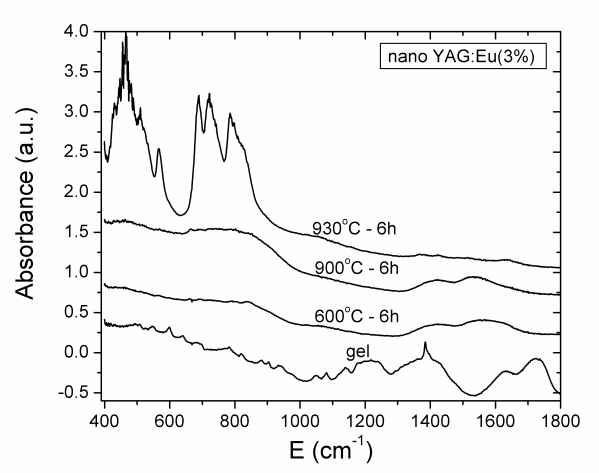

b)

Fig. 3. FT-IR spectra of precursors and nanopowders synthesized at various temperatures. a) YAG:Er nanocrystallites; b) YAG:Er nanocrystallites.

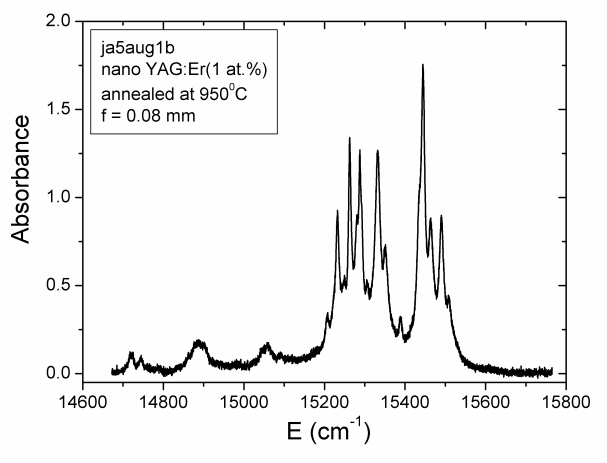

a)

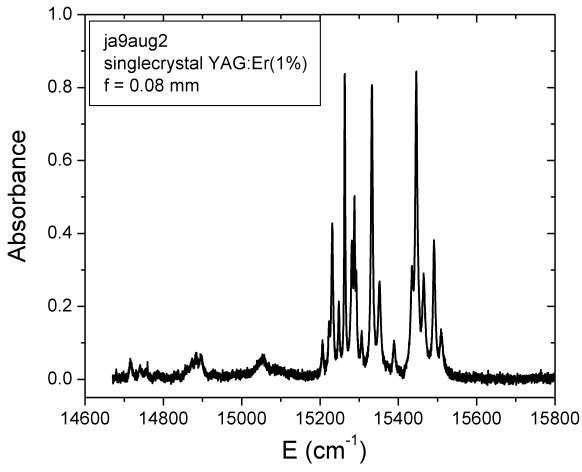

b)

Fig. 4. a) absorption spectrum corresponding to the transition $^4I_{15/2} \rightarrow {}^4F_{9/2}$ in YAG:Er(1 at. %) nanocrystals; b) the same spectrum, but in YAG:Er(1 at. %) bulk crystal.

3.3. Absorption spectra

The absorption spectrum of the transition $^4I_{15/2} \rightarrow {}^4I_{9/2}$ of Er^{3+} in YAG nanocrystals annealed at 930 °C is presented in Fig. 4a. For comparison, it is shown the spectrum of the same transition in a bulk crystal (Fig. 4b). Only the lines corresponding to the garnet phase are present in the Er^{3+} spectrum in the YAG nanocrystals.

3.4. Fluorescence spectra

The amorphous – garnet phase transition is well illustrated with the fluorescence spectra recorded on YAG:Tb (Fig. 5) powders near the transition temperature. At 900 ºC, the fluorescence spectra are characteristic for the amorphous phase (wide fluorescence bands, similar to those observed in glasses) while, after the thermal treatment at 930 ºC, the spectra are representative for the garnet phase. A similar behavior was observed for YAG:Eu [11].

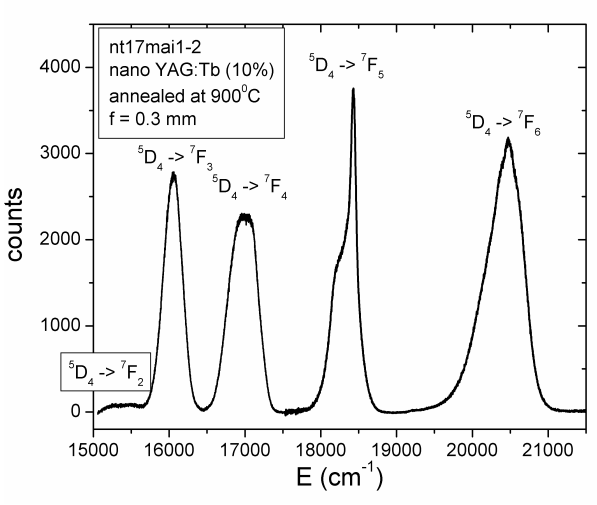

a)

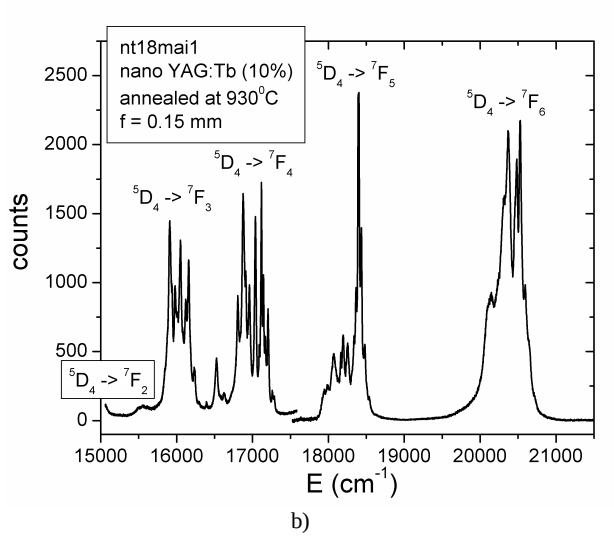

b)

Fig. 5. a) fluorescence spectrum YAG:Tb powder annealed at 900 ℃; b) fluorescence spectrum after thermal treatment at 930 ℃. The spectral domain includes the $^5D_4 \rightarrow {}^7F_J$ (J = 2, 3,…,6) transitions.

Increasing the annealing temperature, the average size of grains increases and the fluorescence lines become narrower (Fig. 6). To illustrate this behavior, we have chosen two isolated fluorescent lines belonging to the $^5D_0 \rightarrow {}^7F_4$ transition of Eu^{3+} in YAG (see the inset in Fig. 6). We interpret this line narrowing as a result of the decreasing of the surface / volume ratio of the crystallites with the increasing size of crystallites. For larger crystallites the ratio surface / volume decreases and the disorder produced by the surface is reduced.

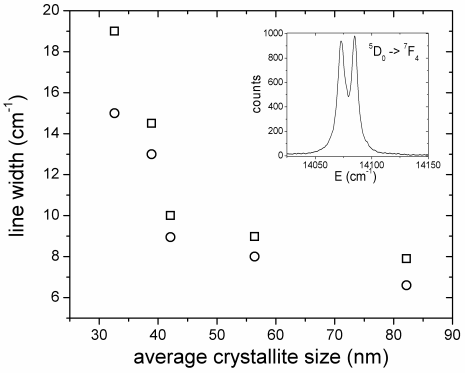

Fig. 6. The effect of the crystallite size on the width of two fluorescent lines of YAG:Eu^{3+} (transition $^5D_0 \rightarrow {}^7F_4$). Squares – the lower energy line in the inset; circles – the higher energy line.

4. Conclusion

In YAG:RE (RE = Er, Eu, Tb) samples prepared by citrate-nitrate sol-gel method the transition from amorphous to crystalline phase takes place in a narrow interval of temperatures (between 900 ºC and 930 ºC).

This phase transition was evidenced using various experimental techniques (XRD, FT-IR and optical spectroscopy). In XRD measurements, it is indicated by the appearance of characteristic YAG lines. The appearance of Y-O vibration lines in FT-IR analysis is also characteristic to this transition, while in optical spectra it is evidenced by the narrowing of the rare-earth emission and absorption lines.

References

[1] A. Ikesue, T. Kinoshita, K. Kamataka, K. Yoshida, J. Am. Ceram. Soc. **78**, 1033 (1995).
[2] J. J. Zhang, J. W. Ning, X. J. Liu, Y. B. Pan, L. P. Huang, J. Mater. Sci. Lett. **22**, 13 (2003).
[3] J. J. Zhang, J. W. Ning, X. J. Liu, Y. B. Pan, L. P. Huang, Mater. Lett. **57**, 3077 (2003).
[4] M. Liu, S. W. Wang, J. Zhang, L. Q. An, L. D. Chen, Key Engineering Materials **280-283**, 517 (2005).
[5] K. Ohno, T. Abe, J. Electrochem. Soc. **133**, 638 (1986).
[6] R. S. Hay, J. Mater. Res. **8**, 578 (1993).
[7] J. J. Zhang, J. W. Ning, X. J. Liu, Y. B. Pan, L. P. Huang, Mater. Res. Bull. **38**, 1249 (2003).
[8] P. Klug, L. E. Alexander, X-ray diffraction procedure, Wiley, New York, 1954, Chap. IX.
[9] J. P. Hurrell, S. P. S. Porto, Phys. Rev. **173**, 851 (1968).
[10] X. Li, H. Liu, J. Wang, H. Cui, Sh. Yang, I. R. Boughton, J. Phys. Chem. Sol. **66**, 201 (2005).
[11] A. M. Chinie, A. Stefan, S. Georgescu, to be published in Rom. J. Phys.

*Corresponding author: anachinie@yahoo.com